Determinants of Allosteric Activation of Yeast Pyruvate Kinase and Identification of Novel Effectors Using Computational Screening[†]

Christopher J. Bond,[‡] Melissa S. Jurica,[‡] Andrew Mesecar,[§] and Barry L. Stoddard*,[‡]

*Graduate Programs in Biomolecular Structure and Design and Molecular and Cellular Biology,
University of Washington and the Fred Hutchinson Cancer Research Center, Division of Basic Sciences,
1100 Fairview Avenue North, Mailstop A3-023, Seattle, Washington 98109, and Department of Medicinal
Chemistry and Pharmacognosy and the Center for Pharmaceutical Biotechnology, University of Illinois
at Chicago (MC 870), MBRB Room 3070, 900 South Ashland Avenue, Chicago, Illinois 60607*

ABSTRACT: We have analyzed the structural determinants of the allosteric activation of yeast pyruvate kinase (YPK) by mutational and kinetic analysis and initiated a structure-based design project to identify novel effectors that modulate its allosteric response by binding to the allosteric site for fructose-1,6-bisphosphate (FBP). The wild-type enzyme is strongly activated by fructose-1,6-bisphosphate and weakly activated by both fructose-1-phosphate and fructose-6-phosphate; the strength of the activation response is proportional to the affinity of the allosteric effector. A point mutation within the 6′-phosphate binding loop of the allosteric site (T403E) abolishes activation of the enzyme by fructose-1,6-bisphosphate. The mutant enzyme is also not activated by F1P or F6P. The mutation alone (which incorporates a glutamic acid that is strictly conserved in mammalian M1 isozymes) slightly reduces cooperativity of substrate binding. Three novel compounds were identified that effect the allosteric regulation of YPK by FBP and/or act as novel allosteric activators of the enzyme. One is a physiologically important diphospho sugar, while the other two are hydrophobic compounds that are dissimilar to the natural effector. These results demonstrate that novel allosteric effectors may be identified using structure-based screening and are indicative of the potential of this strategy for drug discovery. Regulatory sites are generally more divergent than catalytic sites and therefore offer excellent opportunities for discrimination and specificity between different organisms or between different tissue types.

Pyruvate kinase (PK)[1] catalyzes the final step in glycolysis, converting PEP and ADP to pyruvate and ATP. This reaction is a committed step leading to either anaerobic fermentation or oxidative phosphorylation of pyruvate. In most cells, the reaction is essentially irreversible ($K_{EQ} = 2 \times 10^3$ at 30 °C, pH 8.0) and is one of the major control points of glycolysis. The regulation of PK is important for controlling glycolytic flux, which in turn directly effects the concentrations of glycolytic intermediates, biosynthetic precursors, and nucleo-side triphosphates in the cell. Pyruvate kinase also serves as a switch between the glycolytic and the gluconeogenic pathways in certain tissues. The most common form of allosteric regulation for PK is its upregulation by fructose-bisphosphate (FBP), which increases the affinity and reduces the cooperativity of substrate binding. This effect is dependent on bound divalent cations in the active site and is bidirectional: the presence of bound substrate and metal ions also increases the affinity of FBP for the allosteric site.

During fetal development in vertebrates, an allosterically regulatable "M$_2$" isozyme of PK is predominantly expressed. During differentiation, this enzyme is replaced by an unregulated M$_1$ isozyme in most quiescent tissues, while erythrocytes, liver, and cell populations that are not terminally differentiated continue to express allosterically regulated PK isozymes (R, L, and M$_2$, respectively) (*1, 2*). These four PK isozymes are produced by alternative splicing of mRNAs from two separate PK genes. Allosteric regulation of pyruvate kinase appears to be a critical feature of cell cycle progression in rapidly proliferating cells and tissues because PK controls the consumption of metabolic and biosynthetic carbon and the formation of pyruvate for energy production (*1, 2*). Transient upregulation and/or inhibition of glycolysis may occur so that the cellular concentrations of specific metabolites, biosynthetic precursors, and nucleoside triphosphates are driven to appropriate levels at specific points in the cell

* Corresponding author. E-mail: bstoddar@fhcrc.org. Phone: (206)-667-4031. Fax: (206)667-6877.
[‡] University of Washington and the Fred Hutchinson Cancer Research Center.
[§] University of Illinois at Chicago.

[1] Abbreviations: (Y)PK, (yeast) pyruvate kinase; ACD, Available Chemicals Directory; PEP, phosphoenol pyruvate; ADP, adenosine diphosphate; ATP, adenosine triphosphate; 1,6-FBP, fructose-1,6-bisphosphate; 2,6-FBP, fructose-2,6-bisphosphate; F1P, fructose-1-phosphate; F6P, fructose-6-phosphate; T403E, threonine to glutamate substitution at residue 403; BME, β-mercaptoethanol; RBP, ribulose bisphosphate; CPDP, 2-(2-cyanoethenyl)-3-(1-pyrrolyl)-4,6-dimethylthieno[2,3-*b*]pyridine; HPTP, 2-hydroxy-5-(pyrimidine-4-yl)-6-[4-trifluoromethyl)phenyl]-3-pyridinecarbonitrile; DMSO, dimethyl sulfoxide.
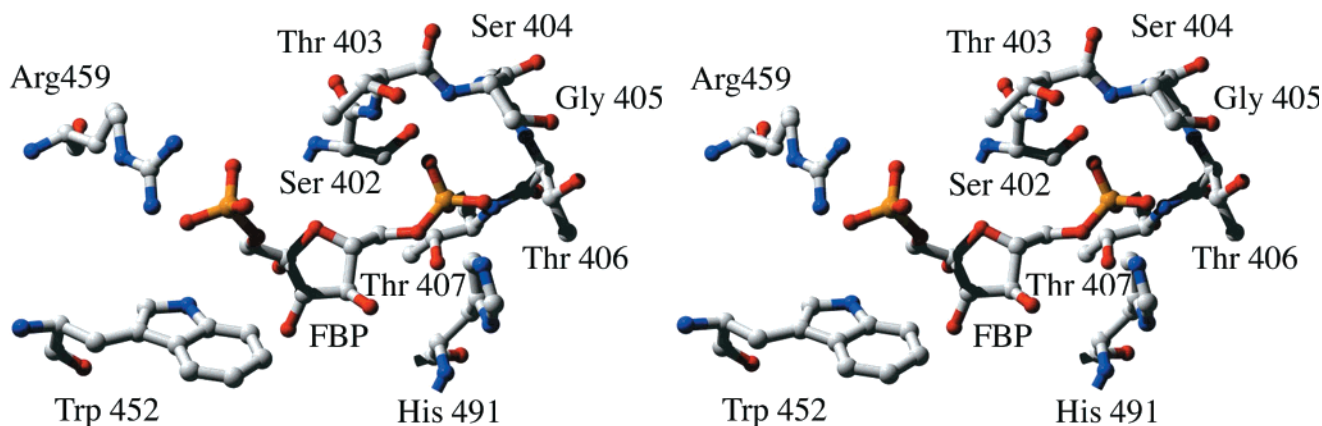
FIGURE 1: FBP binding site in yeast pyruvate kinase. The positive allosteric effector FBP is observed to interact with residues in this binding site through three primary binding determinants: an electrostatic bond between the 1′-phosphate and the side chain of Arg 459; a series of hydrogen bonds between the 6′-phosphate and the serine and side chains of Ser 402, Thr 403, Ser 404, and Thr 407; a combination of van der Waals and hydrogen bond contacts between the ribose sugar and surrounding protein atoms, including Trp 452. Thr 403 is found to be a glutamic acid in all FBP-insensitive M1 PK isozymes sequenced to date.

cycle. This in turn might lead to increased energy production or to increased synthesis of nucleosides and amino acids at appropriate times during cell division.

An example that supports this hypothesis is the observation that solid tumors (which are hyperproliferative, usually hypoxic, and highly dependent on glycolysis) re-express the fetal M_2 isozyme of PK in addition to an increased expression of all glycolytic enzymes and lactate dehydrogenase (*3−6*). This phenomena has been particularly well-documented for human neuroectodermal (brain) tumors (*3*) and breast tumors (*7*). Similarly, a variety of microorganisms that exhibit obligate or facultative anaerobic growth, including bacteria, yeast, and trypanosomes, appear to express only allosterically regulatable forms of pyruvate kinase.

In contrast to active sites, allosteric sites are widely divergent among organisms and even among closely related isozymes within the same organism. This is probably because many forms of enzymatic regulation arose after the initial establishment of catalytic activities in response to the highly specialized biochemical requirements of newly evolved organisms or to the unique metabolic requirements of differentiated tissue types in increasingly complex multicellular organisms. Pyruvate kinase is regarded as an ancient enzyme since it is ubiquitous and highly conserved across all biological groupings. Among all PK enzymes sequenced to date, the residues directly involved in catalysis are almost 100% conserved for all enzyme species ranging from bacteria to humans (*8−10*). In contrast, pyruvate kinase enzymes are regulated by a wide variety of allosteric effectors including fructose-1,6-bisphosphate, fructose-2,6-bisphosphate, L-alanine, and L-phenylalanine or by covalent modification such as phosphorylation (*11−15*). In addition, allosteric sites of PK from different biological species that are regulated by the same effector display a much lower degree of sequence conservation than do their corresponding active sites (*11*). This divergence appears to indicate that regulatory sites might be attractive drug targets for organism-specific and tissue-specific antagonists or deregulators.

The mammalian M_1 and M_2 protein sequences are both encoded by an open reading frame composed of 12 exons and differ by only the alternative splicing of exons 9 and 10 (*16*). These exon regions encode a stretch of 56 amino acids

and comprise approximately 10% of the total protein sequence. Since the M_1 isoform is not allosterically activated by FBP, whereas the M_2 is allosterically regulated by FBP, it is probable this region that contributes residues to the FBP binding site and is important for the different regulatory properties of the enzyme. None of the human PK isozymes has yet been studied crystallographically. The structures of unregulated M1 isozymes from cat (*17−19*) and rabbit (*20*) and allosterically regulated enzymes from *Escherichia coli* (*21*), *Saccharomyces cerevisiae* (YPK) (*22*), and the protozoan *Leishmania mexicana* (*11*) have provided excellent models of the enzyme structure, the organization of the active site, the probable catalytic mechanism, and the binding of 1,6-FBP (*Saccharomyces*). The allosteric site identified by this latter study correlates with the location of residues that differ between the human M1 and M2 isozymes as a result of alternative splicing (*22*).

The allosteric site of YPK (Figure 1) is located 40 Å from the active site and is entirely located within the regulatory C domain. FBP binds in a pocket bordered by two peptide loops made by residues 402−407 (which forms a phosphate-binding region that coordinates the 6′-phosphate of FBP) and 446−452 (which is disordered in the absence of effector but becomes ordered upon binding of FBP). The binding loop for the 6′-phosphate of FBP (residues 402−407) is comprised of residues within the "allosteric exon" in mammalian M_2 isozyme. One residue in this loop (Thr 403) that makes a hydrogen bond to the 6′-phosphate is strictly conserved as a glutamic acid in the unregulated M_1 isozyme in mammals. This observation prompted us to hypothesize that a point mutation (T403E) in YPK might block binding of FBP through steric and electrostatic clashes with the 6′-phosphate, thereby preventing allosteric activation. We have performed a kinetic analysis of activation of the wild-type and mutant enzymes with fructose-1,6-bisphosphate (FBP), fructose-1-phosphate (F1P), and fructose-6-phosphate (F6P). The results of these experiments confirm the structural assignment of the FBP binding site and help define the necessary interactions in this site for allosteric activation. We also report the identification and characterization of three separate compounds that act as weak allosteric activators and also antagonize full activation of enzyme activity by FBP. Two

of these compounds are hydrophobic, aromatic compounds and are unrelated to the natural effector. The third is a diphosphoribosyl sugar that clearly acts in a manner similar to FBP and may be a newly identified, physiological effector of PK in certain organisms.

METHODS

Site-Directed Mutagenesis. A single site-directed mutant of yeast pyruvate kinase where Thr403 was replaced with a glutamic acid was created using the Stratagene QuickChange mutagenesis kit. The following mutagenic primers were synthesized and used to amplify the parent pPYK101 vector: 5′-C-ATT-GTC-TTG-TCC-*GAA*-TCC-GGT-ACC-ACC-CC-3′ and 3′-AG-TAA-CAG-AAC-AGG-*CTT*-AGG-CCA-TGG-TGG-GGT-T-5′. The italicized codon confers the mutation. Parental vector was digested with methylation sensitive restriction enzyme *Dpn*I, while the unmethylated PCR amplified vector remains intact. The vector was transformed into *E. coli*, and the plasmid was prepared from selected colonies. The recovered plasmid was checked by restriction digests, and the PK gene was sequenced to confirm the presence of the mutation. The vector carrying the T403E mutation as well as the wild-type parental vector were then transformed into the *S. cerevisiae* strain PYK1−5 (*a pyk1−5 ade1 leu1 met14 ura3 ade,* Berkeley Yeast Genetic Stock Center), which harbors a mutation that prevents PK expression. This strain cannot grow on glucose as a sole carbon source or on minimal media lacking uracil. Expression of YPK from plasmid pPYK101 confers growth on glucose, thus allowing selection for the plasmid. In addition, this plasmid also has a URA marker so cells transformed with the mutant YPK1 also grow on glucose and media lacking uracil, although at a much slower rate.

Expression and Purification. Pyruvate kinase was purified from *S. cerevisiae* PYK1−5 containing either pPYK101 or the pPYK101 T403E mutant vector using the previously described procedure (22, 23). This yeast strain overexpresses both wild-type and T403E forms of pyruvate kinase when grown in 2% glucose media. Purification of the enzyme involved two chromatography steps, DEAE−cellulose (Sigma) and phosphocellulose (Sigma) and ammonium sulfate precipitation followed by backwashes. Briefly, DEAE−cellulose was equilibrated with 10 mM potassium phosphate, pH 7.0, 5 mM EDTA, and 5 mM β-mercaptoethanol (BME), and cell lysate prepared by osmotic rupture using lyticase was applied. The resin was washed with the equilibration buffer described above, and the effluent solution containing the enzyme activity was then separated and adjusted to pH 6.0 using 1 M HCl. A phosphocellulose slurry in 10 mM potassium phosphate, pH 6.0, 5 mM EDTA, and 5 mM BME was added to the DEAE effluent solution. The phosphocellulose slurry was washed with 10 mM potassium phosphate, pH 6.0, 25% glycerol, 5 mM EDTA, and 5 mM BME. Proteins were then eluted from the column with a linear gradient from 0 to 0.6 M KCl in 10 mM potassium phosphate, pH 6.0, 25% glycerol, 5 mM EDTA, and 5 mM BME. Fractions containing PK were pooled and concentrated to greater than 10 mg/mL. The concentrated protein was then dialyzed overnight against 10 mM potassium phosphate, pH 6.2, 25% glycerol, 5 mM EDTA, and 5 mM BME saturated with ammonium sulfate. The precipitated protein was stored at 4 °C.

Activity Assays. PK activity was measured by a continuous assay coupled to lactate dehydrogenase (LDH) as previously described (23, 24). Activity was measured by the change in absorbance at 340 due to oxidation of NADH by lactate dehydrogenase. Spectrophotometric measurements were made on either a Hewlett-Packard diode array spectrophotometer or on a Cary 100 UV/VIS spectrophotometer with a cuvette holder thermocoupled at 26 °C. Assay conditions were 200 mM KCl, 15 mM MgCl$_2$, 5% glycerol, 100 mM MES (pH 6.2), and 5 mM ADP. FBP and PEP concentrations were varied in these assays. The reaction volume was 2 mL. Reactions were initiated by addition of between 0.01 and 0.04 μg of YPK. Steady-state kinetic rates were determined by measuring the slope of the tangent to the reaction progress curve. Stock substrate concentrations were verified and adjusted using an end point YPK assay by adding an excess of YPK (14 ng) and then measuring the total decrease in absorbance at 340 nm after 5 min. Pyruvate contamination in the PEP stock was measured by adding LDH to the assay buffer and measuring the total decrease in absorbance at 340 nm. The extinction coefficient of NADH used was 6.22 mM^{-1} cm^{-1} . YPK concentrations were used by measuring absorbance at 280 nm and an extinction coefficient of 0.51 (mg/mL)$^{-1}$.

Ligand Binding. Fluorescence binding experiments were performed on a Perkin-Elmer LS50 B luminescence spectrometer. The excitation wavelength was 295 nm with bandwidths of 5 nm for excitation and 5 nm for emission, and fluorescence was monitored from 310 to 400 nm. The cuvette was thermostated at 25 °C. Fluorescence titrations were performed by sequentially adding 5−20 μL of a concentrated ligand solution to 2000 μL of the YPK solution that contained 200 mM KCl, 5 mM PEP, 15 mM MgCl$_2$, 100 mM MES (pH 6.2), 5% glycerol, and 0.082 mg/mL enzyme. The fluorescence signal and ligand concentration were adjusted for the effects of dilution. Fluorescence quenching was calculated from $Q = (F - F_o)/F_o$ where F is the intensity of the fluorescent signal corrected for dilution, and F_o is the signal in the absence of ligand. Dissociation constants were calculated by fitting the quenching data to either of the following two equations:

$$Q = Q_{max}/(1 + K_D/[\text{ligand}]) \qquad (1)$$

or

$$Q = Q_{max}/(1 + (K_D/[\text{ligand}])^{n_H}) \qquad (2)$$

where Q_{max} is the maximal quenching in the absence of ligand, K_D is the apparent dissociation constant for the ligand and n_H is the Hill coefficient. Equation 1 describes a simple binding isotherm with no homotropic cooperativity between subunits, and eq 2 is a form of the Hill equation that describes either positive cooperativity between subunits ($n_H > 1$) or negative cooperativity between subunits ($n_H < 1$).

Computational Database Screening. The basic steps to prepare a ligand screening experiment using DOCK are to identify the target site, to prepare a 3-D model of that site that can be readily compared to 3-D models of superimposed compounds, and to calculate scoring grids that assess and quantitate the potential interaction energy of those compounds to the site. Several reviews and method papers

provide details on the DOCK suite of programs and the general principles of this method (25−28). The YPK structure complexed with the allosteric activator fructose-1,6-bisphosphate (PDB code 1A3W) was used as a search model (22). The model was generated by selecting all YPK residues within 15 Å of the 5′ oxygen of FBP, which is near the center of mass for this compound. Included in this model were the side chains that contact the 1′-phosphate of FBP (Arg 459), the 6′-phosphate (Ser 402, Thr 404, and Thr 407), and the ribose sugar ring and its 3′- and 4′-hydroxyls (Trp 452 and the backbone amide groups of residues 483 and 491, respectively). After removal of bound FBP, a molecular surface representation of the binding site was generated using MIDAS (29). Subsequently, a sphere set (which fills the binding site and represents its "negative" 3-D image) was generated using the DOCK SPHGEN routine. All molecular surface points were used in the calculation of the sphere set. A "dotlim" value (which defines how finely local invaginations of the molecular surface are sampled) of −1 was used. The maximum sphere radius was 4.0 Å, and the minimum was 1.4 Å. Spheres output by SPHGEN that were outside the known FBP binding pocket were rejected, leaving a total of 39 spheres to define the allosteric binding site. The maximum distance between intraligand and intrareceptor points (which serves as a cutoff for scoring superimposed ligand atoms and receptor spheres as "equivalent") was set to 0.25 Å. Six of the 39 spheres were designated "critical" to force at least one atom in every docked ligand orientation to be near the bound position of the 1′-phosphate in FBP.

Precalculated energy grids, which are used to calculate the energy score for any ligand−receptor atom pair in the docked solutions, were generated by the DOCK routine GRID. Atomic partial charges were assigned to the receptor site prior to calculating these grids using the MOPAC semiempirical quantum mechanics package in QUANTA (30). Hydrogen atoms were assigned to the receptor site for assignment of grid partial charges and van der Waals radii. Hydrogen atoms were built with the protein design application in QUANTA; the pH of the receptor was assumed to be 7.0. For the generation of grids, a united atom model in which hydrogens attached to carbons are assigned a zero van der Waals well-depth and the partial charge is transferred to the carbon was used. Grid spacing was set at 0.2 Å, and the nonbonded scoring cutoff distance was set to 10 Å. The intermolecular interaction energies were modeled using a combined van der Waals and electrostatic interaction potential. Electrostatic interactions were modeled using a distance-dependent dielectric and an initial dielectric constant of 4. The energy grid was superimposed on a bounding box 19.6 × 24.1 × 17.0 Å. There were 1 062 864 points in the final energy grid.

DOCK version 4.0.1 was used to screen against all the molecules in the 1997 release of the Available Chemicals Database (ACD) (31). The ACD contains 370 000 unique compounds broken up into 23 individual files. Only compounds with 10−35 heavy atoms were used in the screen. The database was screened twice; once using both electrostatic and van der Waals terms and a second time using only van der Waals interaction terms as a test for shape complementarity. Only rigid ligand models were used in the screen due to computational time restraints. A maximum of 100 orientations was generated for each ligand. The potential energy of each orientation was subsequently minimized using the default SIMPLEX minimizer in DOCK. Initial transitional and rotational step sizes were set to 1 Å and 18.0 deg, respectively. The maximum number of iterations was set at 100. If the energy of minimized orientations varied less than 0.1 kcal/mol, then the minimization was terminated. One cycle of minimization was performed for each compound. The ligands and their associated orientations with the best 200 scores from each dock run were saved for visual inspection. The DOCK runs were performed on a Silicon Graphics R10000 Origin work station with 230 mByte memory running IRIX 6.3; each run took approximately 8 h.

An initial list of top DOCK solutions was compiled by combining top scoring compounds from both screens and eliminating redundant listings. This resulted in a docked list of 5,698 compounds. The large number of compounds from the DOCK screen mandated that visual classification be based upon simple rules that allowed for rapid screening. Three rounds of visual inspection were performed to reduce the total number of compounds for kinetic screening and further analysis. Compounds were selected such that a significant degree of chemical diversity would be represented. After these rounds of manual assessment, the number of candidate compounds was reduced to 42, and these compounds were assayed for modulation, i.e., activation or inhibition, of PK activity. The final list of compounds assayed represented 11 distinct chemical classes that are summarized in the Results.

Kinetic Screens of Selected Compounds. The compounds selected for further kinetic analysis were purchased from a variety of vendors. Compounds were prepared for the initial multisample kinetic screen at a concentration of 3 mM by dissolving in 100 mM MES, pH 6.2. Compounds that did not readily dissolve under these conditions were centrifuged to pellet the insoluble fraction, and the supernatant was used at the apparent solubility limit in this buffer. Once prepared, compounds were used immediately to minimize any solvent-mediated breakdown. These compounds were then screened in a multisample kinetic assay for modulation of PK activity. The assays were performed both in the presence and in the absence of the physiological FBP effector, as described below.

PK activity was measured in all kinetic experiments by a continuous assay coupled to lactate dehydrogenase (LDH) as described above, modified for screening multiple samples simultaneously. Spectrophotometric measurements were made on a 96-well Molecular Devices VersaMax microplate reader at ambient temperature for the multicompound screens. Assay conditions were 200 mM KCl, 15 mM $MgCl_2$, 5% glycerol, 100 mM MES (pH 6.2), and 5 mM ADP. The PEP concentrations were fixed at 750 μM, because PK activity is strongly dependent on the presence or absence of bound effector at this concentration. FBP and DOCK compound concentrations were varied in the assays. The reaction volume was 100 μL for the multiplate kinetic assays. Reactions were initiated by addition of between 0.01 and 0.04 μg of YPK. Path lengths in the 96-well plate reader were measured by using an internal standard concentration of bromophenol. The absorbance of the 100-μL standard concentrations were measured and then compared to the absorbance of the same standard concentration measured in

Table 1: Steady-State Kinetic Parameters of Pyruvate Kinase Activation

	wild-type			T403E		
	$K_d{}^a$ μM^c	K_m (PEP) (μM)	$n_H{}^b$	K_d (μM)	K_m (PEP) (μM)	$n_H{}^b$
no effector		1150 ($\pm$ 7)	3.7 ($\pm$ 0.06)		960 ($\pm$ 80)	2.7 ($\pm$ 0.2)
FBP	10	50 ($\pm$ 0.5)	1	>5400	830 ($\pm$ 60)	2.6 ($\pm$ 0.04)
F1P	490	271 ($\pm$ 21)	2.1 ($\pm$ 0.2)	>7500	834 ($\pm$ 16)	2.8 ($\pm$ 0.1)
F6P	1300	410 ($\pm$40)	3.2 ($\pm$ 0.3)	>7500	960 ($\pm$ 80)	2.7 ($\pm$ 0.2)

[a] Determined by tryptophan titrations of YPK in the presence of 200 mM KCl, 5 mM PEP, and 15 mM $MgCl_2$, pH 6.2. Data were fit to either eq 1 or eq 2 described in Methods. All data were best fit to eq 1 where $n_H = 1$, indicating no homotropic cooperativity in binding. [b] The Hill coefficient n_H was determined from fits of the kinetic data to the Hill equation. [c] The dissociation constant for FBP was taken from a previous study (15) and was measured with Mn as the divalent cation.

a 1-cm cuvette. Sets of seven compounds were assayed simultaneously across the 96-well plate in the presence and absence of FBP. For each compound, the assays were performed in triplicate: three wells were assayed without FBP, and three were assayed with FBP. A compound was judged to be active in this assay in either of the two following situations: PK activity decreasing in the presence of FBP was interpreted as the compound interfering with FBP-dependent activation; PK activity increasing in the absence of FBP was interpreted as the compound acting as an activator of the enzyme. For any such compound, controls were performed to ensure that the compound was not interacting directly with the assay's coupling enzyme (lactate dehydrogenase).

Three compounds were found to significantly modulate PK activity and were thus characterized further. These compounds were ribulose-1,5-bisphosphate; (Sigma Inc. Catalog No. R0878), 2-(2-cyanoethenyl)-3-(1-pyrrolyl)-4,6-dimethylthieno[2,3-*b*]pyridine (CPDP; Bionet Inc. Catalog No. 4K-027), and 2-hydroxy-5-(pyrimidine-4-yl)-6-[4-tri-fluoromethyl)phenyl]-3-pyridinecarbonitrile (HPTP; Peakdale Inc. Catalog No. PFC-0591). 1-D NMR spectra were collected on these compounds in order to confirm the identity and purity of the samples. Spectra were taken on a DRX 499 spectrophotometer with an Oxford 11.7 T superconducting magnet and a 5-mm probe. RBP was dissolved in D_2O at 1 mM, CPDP and PFC were dissolved in deuterated DMSO $((CD_3)_2SO)$ at 1mM. Spectra were taken at 25 °C. A scanwidth of 0−10 ppM was used.

Analysis of Novel Effectors. For kinetic and binding assays, ribulose-1,5-bisphosphate was prepared as a 100 mM stock in water. The other two (CPDP and HPTP) exhibited limited solubility in aqueous solution and were therefore prepared as stock solutions in DMSO at 26.5 and 85.3 mM concentrations, respectively. DMSO alone was assayed in the kinetic protocol described below to ensure that it does not by itself cause a change in the kinetic profile of the enzyme. For CPDP and HPTP, cuvettes with 2-mm path lengths were used to decrease the total absorbance signal because the effectors absorb in the same range as NADH.

Dissociation and activation constants were determined for the three lead compounds using a combination of three methods: intrinsic YPK tryptophan fluorescence as described above (for RBP, which does not possess a strong inherent fluorescence signal), the response of YPK activity to ligand concentration in the absence of FBP (for HPTP and CPDP), and equilibrium dialysis (for HPTP). Activation constants for CPDP were determined by measuring YPK activity as a function of ligand concentration. PK activity versus the concentration of ligand concentration was fit to ($\nu = V_{max}(1$
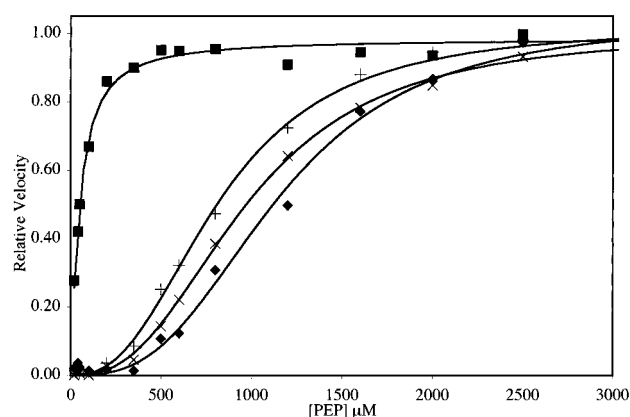

FIGURE 2: Substrate velocity profile for wild-type and T403E mutant PK in the presence and absence of 1 mM FBP. Values shown are averages ($n = 3$): ($\blacklozenge$) wild-type + 0 mM FBP; ($\blacksquare$) wild-type + 1 mM FBP; ($\times$) T403E + 0 mM FBP; (+) T403E + 1 mM FBP. Data were fit to the Michaelis−Menten or Hill equations, and the resulting kinetic parameters are summarized in Table 1.

$+ (K_A/[\text{ligand}])n_H))$, where $\nu = (v - v_0)/(v_{max} - v_0)$ and v_0 is the enzyme velocity in the absence of effector. Activity titrations were performed under the kinetic conditions described above; PEP concentrations were fixed at 350 μM. All curves were fit using Table 2D (SPSS Scientific Inc., Chicago, IL). Equilibrium dialysis binding measurements were performed by dialyzing 150 μL of YPK buffer containing 13 μM YPK against 40 mL of reaction buffer containing 25 μM HPTP. Concentrations of HPTP were measured by absorption at 345 nm. Compounds were allowed to dialyze for 3 days. No difference was seen in control experiments where enzyme was withheld from the binding solution.

RESULTS

Effector Binding and Kinetic Effects. Binding and activation of wild-type and T403E mutant yPK were characterized both by substrate velocity assays and by intrinsic tryptophan fluorescence (Table 1, Figure 2). Tryptophan 452 is located in the allosteric effector binding site, and it is the only tryptophan residue in a single YPK subunit. Its fluorescent signal is very sensitive to binding interactions at that site (24). In the absence of the allosteric activator FBP, mutation of threonine 403 to glutamic acid does not significantly alter the affinity of YPK for the substrate PEP (the K_M for PEP substrate is 960 $\pm$ 80 μM for the mutant vs 1150 μM for wild-type), but the mutation does slightly reduce cooperativity of substrate binding (the Hill coefficient for T403E is 2.7 in the absence of effector as compared to a value of 3.7
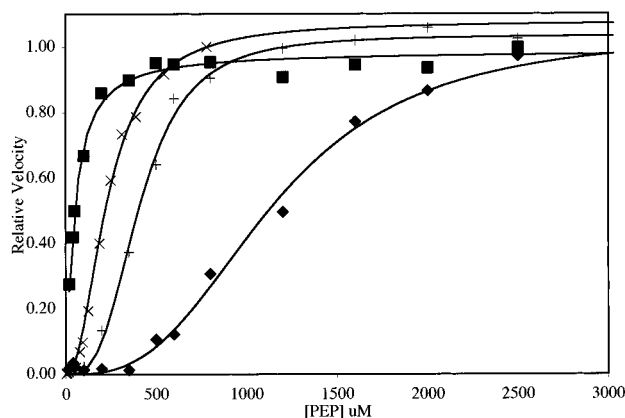
FIGURE 3: Substrate velocity profile for wild-type enzyme. (◆) No effector present; (■) 1 mM FBP; (×) 2 mM F1P; (+) 5 mM F6P. Data were fit to the Michaelis−Menten or Hill equations, and the resulting kinetic parameters are summarized in Table 1.

for wild-type). As predicted on the basis of previous crystallographic studies, the mutation strongly interferes with both binding and activation of the enzyme by fructose-1,6-bisphosphate. The K_d of the wild-type enzyme for FBP is 10 μM whereas the same value for the T403E enzyme is greater than 5400 μM. Addition of saturating levels of FBP to wild-type YPK reduces the K_m value of PEP from 1150 to 50 μM and its Hill coefficient from 3.7 to 1.0. In contrast, the mutant is not significantly activated by FBP even at millimolar concentrations. The K_m (PEP) exhibited by T403E in the absence of FBP is 960 $\pm$ 80 μM; addition of 1 mM FBP gives a K_m value of 830 $\pm$ 60 μM. We attribute the small decrease in substrate affinity of T403E, when assayed in the presence of high levels of FBP, to a weak interaction of the effector with the allosteric site that results from an altered conformation that precludes its interaction with the mutated 6′-phosphate binding loop of the enzyme.

The wild-type enzyme is weakly activated by both F1P and F6P (Table 1, Figure 3). Tryptophan fluorescence titrations of the enzyme indicate that F1P and F6P bind with modest affinity to the FBP site, and their affinity is increased by the presence of divalent cations as is also observed for FBP (data not shown) (23). The dissociation constant of the wild-type enzyme for F1P is 490 μM and for F6P is 1300 μM. In the presence of 2 mM F1P, K_M (PEP) is reduced to 271 μM, and the Hill coefficient is reduced to 2.1. In the presence of 5 mM F6P, the K_M value for PEP is reduced to 410 μM, and the Hill coefficient is reduced to 3.2. Therefore, the strength of allosteric response of YPK to these compounds is observed to be FBP $\gg$ F1P > F6P, matching their relative affinities for the allosteric binding site. The T403E enzyme mutant displays greatly increased dissociation constants for all three effectors as compared to wild-type enzyme (>5400 μM for FBP, >7500 μM for F1P and F6P). The kinetic profile of the enzyme mutant T403E resembles the low-affinity, unactivated wild-type enzyme; it is not significantly activated by any of these compounds (Table 1). Of these three compounds, F6P is the poorest activator of the T403E mutant.

Initial DOCK Screens. In each DOCK screen, the top 200 scoring ligands from each ACD section were selected. Fructose-1,6-bisphosphate is present in the ACD and served as a positive control for the DOCK screens. Both screens, using van der Waals contact scoring only or contact plus

electrostatic terms, identified FBP as a possible ligand. FBP was present in the top 200 scoring ligands relative to the ~15,000 other compounds in its section of the ACD.

The final list of compounds that appeared reasonable as docked ligands to the PK allosteric site was composed of 42 compounds from 11 distinct chemical classes. Overall, most of the compounds contained one or two polar moieties, but few had an overall net charge other than zero. The protein−ligand contacts for various docked compound orientations were distributed fairly evenly throughout the target cleft. Compounds were selected that filled at least the two or more pockets defined by the 1′- and 6′-phosphates and the ribose sugar ring of bound FBP and an additional cleft near Arg 425 that is not occupied by FBP. The largest class of compounds identified in the searches were benzene derivatives. The compounds selected from this class included those with 1−5 substituents, many of which were branched. The principle docked location of the benzene ring was in the large pocket filled by the 6′-phosphate, which is slightly removed from the cavity occupied by the sugar ring of FBP. Only one derivative made significant contacts with Trp 459. Other compounds in the library included esters, heteroalkenes, small peptidomimetics, several small phosphate-containing compounds, complex amines, substituted sugars, and sulfones.

Of the 42 compounds tested for modulation of PK activity, 14 appeared to measurably affect the activity of YPK under the conditions used for the assay. Four compounds antagonized the effect of FBP, reducing the activity of YPK in the presence of 1 mM FBP. Nine reduced the activity of YPK in the absence of FBP, and one acted as an FBP mimic (increasing the reaction velocity in the absence of FBP). Of these compounds, three were selected for further characterization (Figure 4). One was a diphospho sugar similar to FBP (ribulose-1,5-bisphosphate), and two (CPDP and HPTP) were complex amines that were relatively hydrophobic and had little similarity to the natural allosteric activator. The identity and purity of each compound was verified by 1-D NMR.

Active Compounds. A summary of the binding affinities and kinetic parameters for the compound described below are provided in Table 2. One of the compounds identified by DOCK and shown to act as an allosteric activator was a 5-carbon, open-chain sugar with two terminal phosphate groups, ribulose-1,5-bisphosphate (RBP). This compound is chemically similar to the physiological activator fructose-1,6-bisphosphate, although it is modeled in an open chain conformation in the ACD and appears to exist primarily in that form in solution as shown by NMR spectra (data not shown). The highest scoring binding mode for RBP is similar to that determined crystallographically for FBP, with the 1′- and 5′-phosphates interacting with Arg 459 and the phosphate binding loop formed by residues 402−407 (Figure 4b). The dock score for both van der Waals and electrostatic interactions is −56.6 kcal/mol for RBP as compared to −63.0 for FBP; both are well above the mean score for that section of the ACD. RBP activates YPK by shifting the low-affinity, cooperative kinetic profile for PEP to a higher affinity, less cooperative state, albeit to a lesser extent than FBP (Table 2, Figure 5). RBP binds with a K_D of 570 μM as compared to a K_D of 10 μM for FBP. The enzyme's K_M for PEP is reduced from 1150 to 450 μM upon addition of 3 mM RBP
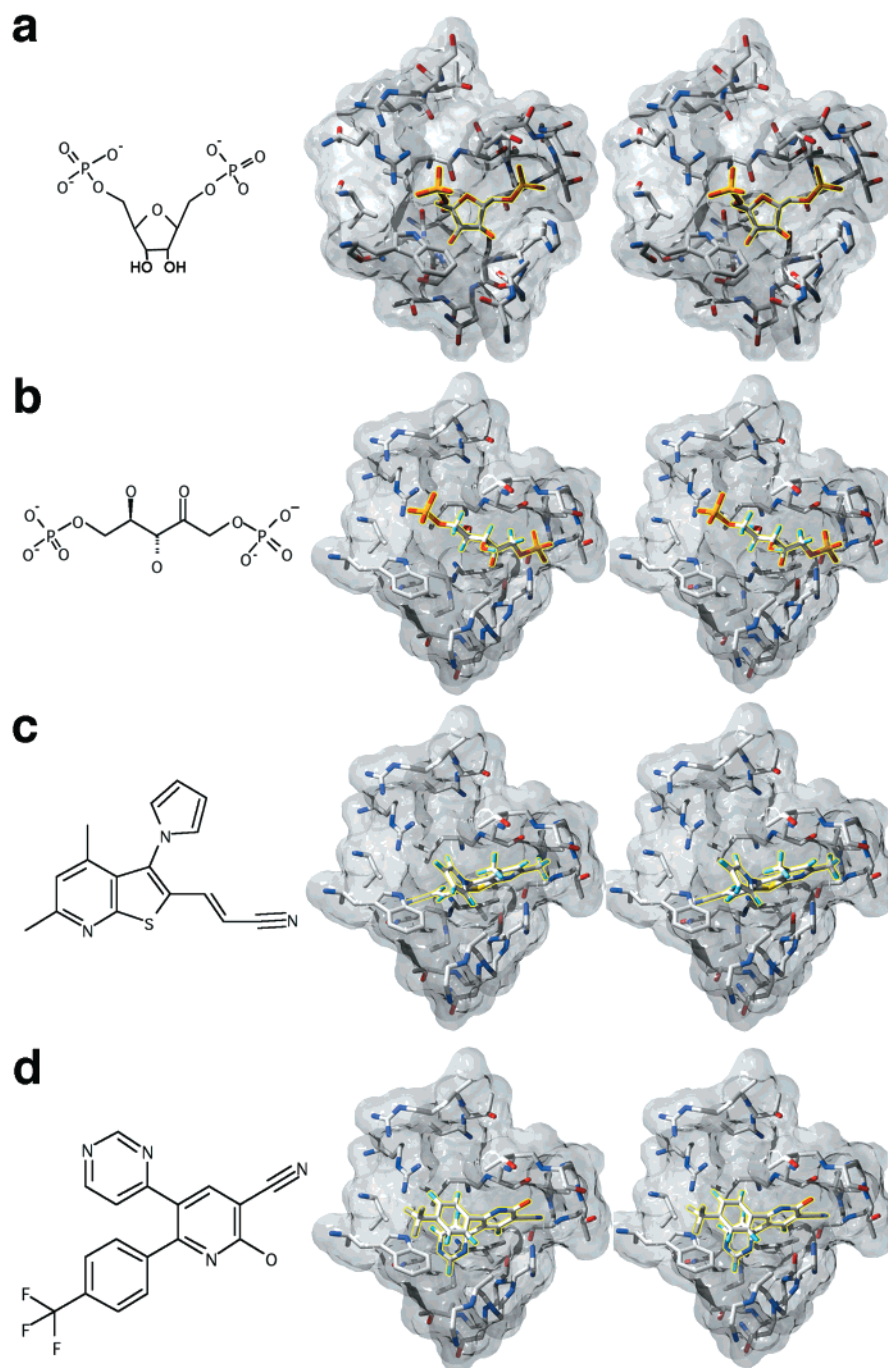
FIGURE 4: Chemical structures and bound orientations of (a) fructose-1,6-bisphosphate; (b) ribulose-1,5-bisphosphate; (c) CPDP; and (d) HPTP. The molecular surface of the binding site is shown as a semi-transparent gray surface covering the protein atoms that comprise the site; the four panels are shown in the same orientation. The bound position of FBP was crystallographically determined; the positions of the latter three compounds are those predicted by DOCK. Stereoview of the molecular surface of the allosteric binding site in YPK. Note that FBP does not completely fill the available space within the allosteric binding site. Note also the similarity in positions of the terminal phosphates of RBP to those in the crystal structure of bound FBP.

whereas 1 mM FDP reduced the K_M for PEP to 50 μM. The Hill coefficient of PEP is also reduced by RBP to an intermediate value of 1.62 as compared to a value of 1.0 produced by FBP. The values for the Hill coefficients indicate that the cooperativity of PEP binding is reduced but not eliminated by RBP.

RBP quenches the intrinsic tryptophan fluorescence of YPK as does FBP (data not shown). Only one tryptophan residue (Trp 452) exists in the YPK sequence, and it is located in the allosteric effector binding site. The effective quenching of Trp 452 by RBP strongly suggests that this

compound also binds in the FBP binding site. Trp 452 makes a direct contact with FBP and this interaction is most likely the mechanism for the quenching and spectral shift in the emission spectrum (*34*). Furthermore, RBP mediated quenching is strongly dependent upon the presence of Mg^{2+}, as is also observed for FBP (*34*). In the presence of 15 mM Mg^{2+}, RBP binds with a K_D of 500 μM; in the absence of Mg^{2+}, the K_D is on the order of 10 mM.

A second compound (2-(2-cyanoethenyl)-3-(1-pyrrolyl)-4,6-dimethylthieno[2,3-*b*]pyridine or CPDP) was also shown to allosterically activate YPK. CPDP is a 15-carbon complex

Table 2: Binding Constants and Kinetic Parameters for PK Allosteric Effectors[a]

	K_d (μM)	K_m (PEP) (μM)	n_H (Hill coeff)
no effector		1150 ($\pm$ 70)	3.7 ($\pm$ 0.6)
FBP	10 ($\pm$ 1)	50 ($\pm$ 0.5)	1.0
RBP	570 ($\pm$ 4)	450 ($\pm$ 10)	1.6 ($\pm$ 0.12)
CPDP	7.6 ($\pm$ 4)	820 ($\pm$ 37)	2.7 ($\pm$ 0.5)
HPTP	77 ($\pm$ 2)	620 ($\pm$ 12)	1.3 ($\pm$ 0.16)

[a] Steady-state kinetic parameters K_M and n_H determined in the presence of the following concentrations of effector: 1 mM FBP, 3 mM RBP, 100 μM CPDP, and 400 μM HPTP. Binding constants determined as describe in Results.
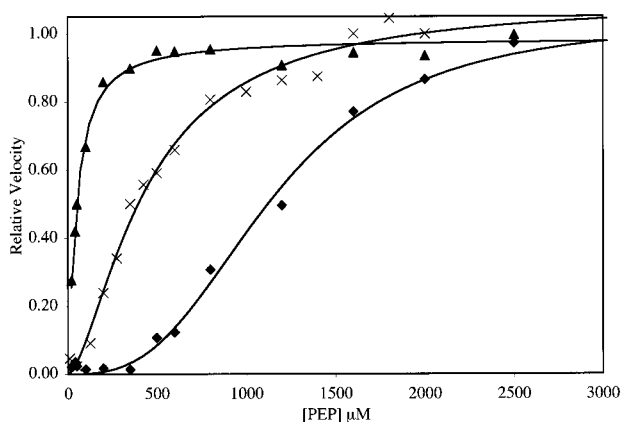

FIGURE 5: PEP-dependent kinetic profile of wild-type yeast pyruvate kinase in the presence of FBP vs RBP. Velocities were measured in the presence of 1 mM FBP (▲), 3 mM RBP (×), and in the absence of effector (◆). PK activity in the presence of FBP was fit to the Michaelis−Menten equation. Activity of the enzyme alone or in the presence of RBP were fit to the Hill equation to allow calculation of cooperativity. Similar analyses were performed for CPDP and HPTP; the resulting values for effector binding constants, substrate K_m, and cooperativity are summarized in Table 2.

amine, molecular weight of 279. CPDP is quite hydrophobic as the cyano moiety is the only polar group on the compound. As a result, solubility of this compound is limited in water to approximately 30 μM. The docked and minimized model of bound CPDP is shown in Figure 4c. The 4-methyl group of the pyridine ring is located in the pocket formed by residues 402−407, which bind the 6′-phosphate of FBP. The cyanoethenyl tail of the molecule is buried underneath Trp 452, and the pyrroyl ring is largely solvent exposed and contacts the outer face of Trp 452. The dissociation constant of CPDP from YPK is 15 μM, as determined by activity titrations and equilibrium dialysis. CPDP binding is considerably tighter than RBP, and its K_D value is near the K_D value of FBP (10 μM). The K_M for PEP shifts from 1150 μM in the absence of effector to 820 μM in the presence of 27 μM CPDP, and the Hill coefficient decreases from 3.7 to 2.7 (Table 2). Although CPDP binds ∼40-fold more tightly than RBP and with a similar affinity as FBP, it is a weaker allosteric activator of PEP binding than RBP. This compound does not measurably activate the allosteric site mutant of YPK (T403E).

A third compound (2-hydroxy-5-(pyrimidin-4-yl)-6-[4-(trifluoromethyl)phenyl]-3-pyridinecarbonitrile, HPTP) also acts as an effector that weakly activates the enzyme. Like CPDP, HPTP is a complex hydrophobic amine with a molecular weight of 342. The docked and minimized model

of bound HPTP is shown in Figure 4d. The hydroxyl group fits into the pocket defined by residues 402−407 that normally bind the 6′-phosphate of FBP, while two of the three aromatic rings fill the central sugar pocket. The trifluorophenyl group packs on top of Trp 452 and is partially solvent-exposed. HPTP is slightly more soluble that CPDP, and it exhibits a solubility limit in water of ∼850 μM. HPTP binds to YPK with a dissociation constant of 77 μM, as determined by activity titration and by equilibrium dialysis. Like CPDP, HPTP binds with a similar affinity as the physiological FBP effector and effects both the affinity and cooperativity of PEP binding (Table 2). The K_M of PEP is reduced from 1150 to 450 μM by the addition of 500 μM HPTP, and the Hill coefficient is reduced from 3.7 to 1.6. Unlike CPDP and FBP, HPTP activates T403E reducing its K_M from 960 to 650 μM and shifting the enzyme toward a less cooperative state.

DISCUSSION

In this study, we report the effect of a point mutation (T403E) in yeast PK to block binding of FBP and hence activation of the enzyme. We also describe the effect of removing the 1′- or 6′-phosphate from the allosteric effector on its binding and enzyme activation. These experiments allow us to verify the location of the FBP binding site previously visualized by crystallographic analysis, to characterize and quantitate the relative contribution of the individual phosphate groups of FBP to binding, and to measure the relationship between effector affinity and the strength of allosteric activation. Using this same enzyme, we also demonstrate that structure-based, computational screening methods, previously shown to be powerful tools for the discovery of active-site inhibitors, can also be used to select novel ligands for allosteric regulatory sites. Such sites may present novel targets for drug design because of their inherent structural divergence among various organisms and tissue types. In the case of pyruvate kinase, a variety of regulated forms of the enzyme has evolved to meet the specific metabolic requirements of the source organism or tissue. While deregulation of enzymatic function might produce more subtle effects on enzyme kinetics than complete inhibition, such an effect might cause profound metabolic and cellular responses in vivo.

Effector Binding and Kinetic Effects. FBP binds to the allosteric site of YPK with a dissociation constant of 10 μM, appropriate for a metabolic intermediate that also acts as an enzyme regulator. The allosteric site of yeast pyruvate kinase is located 40 Å from the active site and is entirely located within the regulatory C domain (*22*). FBP binds in a pocket formed by two loops composed of residues 402−407 and 446−452. This second loop is disordered in the absence of effector but becomes ordered upon binding of FBP. The FBP binding pocket is largely polar and basic, complementing the net negative charge of FBP. The strongest interactions stabilizing the effector complex appear to be direct polar interactions between the enzyme and the 1′- and 6′-phosphate groups of FBP. These contacts include a 2.8-Å salt bridge between the 1′-phosphate and the Arg 452 side chain; the 6′-phosphate of FBP forms a series of polar interactions with side chains Ser 402 (2.6 Å), Ser 404 (3.3 Å), and Thr 407 (2.5 Å). In addition, the 3′- and 4′-hydroxyls of the fructose ring contact the backbone carbonyl oxygen of residue 483

and the backbone nitrogen of residue 491, respectively. The single tryptophan per enzyme subunit (Trp 452) is solvent-exposed in the absence of effector and is largely buried by the fructose ring of bound FBP (average distance ~4 Å). Binding of FBP attenuates the fluorescent profile of YPK through its interactions with Trp 452.

Removal of the 1′- and 6′-phosphate groups of FBP, generating F6P and F1P, respectively, leads to significant increases in the dissociation constants of the effectors to YPK. The K_D for F1P (490 μM) is 49-fold higher than for FBP, while the corresponding K_D for F6P (1300 μM) is 130-fold times higher. On the basis of these observations, it appears that the salt bridge from Arg 452 to the 1′-phosphate of FBP contributes between 2- and 3-fold greater binding energy than the interactions between the 6′-phosphate and residues Ser 402, Ser 404, and Thr 407. Kinetic analyses of enzyme activation, conducted at saturating concentrations of F1P and F6P, indicate that both effectors weakly activate the enzyme. Under these conditions, the K_M for PEP substrate is decreased from 1150 to 271 μM, with F1P as an activator, and to 410 μM with F6P as an activator. The cooperative binding of substrate is also diminished, although not as dramatically as by FBP. Overall, the strength of the allosteric response decreases as the affinity of the effector decreases. Our interpretation of this result is that strong allosteric activation of YPK requires the formation of fully ordered interactions with both phosphate groups of the effector in order to induce the full conformational change that results in an increase in PEP affinity at the active site.

The nature and magnitude of the allosteric conformational transition in pyruvate kinase is somewhat unclear. Structural studies of the unactivated and uncomplexed *E. coli* enzyme have led to a hypothesis that binding of FBP induces rotations of the catalytic and C-terminal domains by 17 and 15°, respectively, relative to the principle symmetry axes of the enzyme tetramer (*12, 21*). This proposed motion is thought to involve shearing and rotational motions of several α-helices at the tetramer interfaces between the allosteric and active sites. It was further proposed that residues at the subunit interfaces participate in allosteric communication by facilitating these motions and coupling conformational changes in the allosteric site to corresponding conformational changes in the active site. The structure of yeast PK complexed with the allosteric activator FBP indicated that binding of the effector might induce movement of the Cα2 helices (residues 378−393) in the tetramer interface, primarily through the association of the 6′-phosphate with residues 402−407 and bending of a β-strand that connects those residues to the Cα2 helix (*22*). A subsequent crystallographic study from *L. mexicana*, however, indicated that the magnitude of conformational domain motions induced by effector binding might be considerably smaller because the structure of that enzyme in the absence of a bound substrate and allosteric effector closely resembled the yeast enzyme−FBP complex and the nonallosteric muscle enzymes (*11*). A definitive resolution of these models awaits the structure determination of an unactivated and fully activated enzyme from the same biological source.

The kinetic profile of the enzyme mutant T403E resembles the low-affinity, unactivated wild-type enzyme, although with a slightly lower Michaelis constant for PEP (T403E, 960 ± 80 μM, vs wild-type, 1150 ± 7 μM) and a slightly lower

degree of substrate binding cooperativity (T403E Hill coefficient, 2.7 ± 0.2, vs wild-type, 3.7 ± 0.06). The substitution made by this mutation places a negatively charged glutamate side chain directly within the 6′-phosphate binding pocket of YPK. This residue is a glutamate in all of the unregulated (FBP-insensitive) M1 isozymes sequenced to date. The T403E mutant enzyme is not strongly bound or activated by any of the effectors discussed above (FBP, F1P, or F6P), and of these compounds, F6P appears to be the least capable of inducing any shift in the kinetic profile of the enzyme.

On the basis of these observations, we draw several conclusions: (i) The presence of the glutamate carboxylate group in the allosteric site of YPK may by itself slightly nudge the conformational equilibrium of the enzyme tetramer toward an "activated" state. (ii) The presence of glutamate 403 prevents binding of effectors through a combination of steric clash and electrostatic repulsion. F6P appears to be completely inhibited from binding the mutant enzyme, while FBP and F1P may act as very weak activators, presumably by interacting with the allosteric site in a manner that precludes contacts with the pocket formed by residues 402−407. The observation that F1P (which lacks a 6′-phosphate) binds and activates the mutant as poorly as FBP may imply that the reduction in the overall positive charge of the allosteric pocket by the T403E mutation is sufficient to inhibit binding, even in the absence of direct steric clash. (iii) Full activation requires binding of allosteric effector rather than the simple presence of a negative charge in this pocket (such as the carboxylate of Glu 403). Past studies have shown that the effector must be in the correct stereochemical conformation (the β-anomer in the case of FBP) in order to promote binding and activation (*32−34*). (iv) The presence of a glutamate at this position in unregulated M1 isozymes cannot by itself account for the high-affinity, noncooperative kinetic response of those species. For those PK isozymes that differ only by an alternatively spliced exon (such as mammalian M1 and M2 isozymes), multiple residues from that region probably act in concert to impart novel regulatory properties to each enzyme species.

Structure-Based Screening Methodologies against Allosteric Sites. Our approach to searching for novel allosteric ligands was to screen the ACD using a computational search and then to perform a low throughput, kinetic screen of the candidate compounds after they were reduced to a tractable number. The YPK system represents an interesting challenge for a number of reasons. First, the natural effector (FBP) is highly charged, and it binds to a relatively basic binding cleft via interactions that are highly polarized between the effector and protein side chains. Since compounds under consideration as drug candidates should usually be capable of diffusion across lipid bilayers, it was our goal to identify compounds that could modulate PK activity but display no net charge or readily ionizable groups. Thus, the desired compounds should possess significantly different chemical features and solution behavior than the natural effector while still displaying structural complementarity against its binding site. Second, the dissociation constant for 1,6-FBP from the allosteric site of YPK is 10 μM, which is reasonable for a glycolytic intermediate that also acts as a metabolic regulator. It therefore seemed possible that an initial screen of compounds would identify one or more lead compounds that would have affinities approaching that of FBP. With affinities

Bond et al.

in the mid-micromolar range for CPDP and HPTP, this hypothesis was correct. Finally, a kinetic assay and screen designed to identify compounds that modulate enzymatic activity through allosteric interactions is designed in a slightly different manner than an assay designed to identify competitive inhibitors. It is necessary for such screens to exploit conditions that place the enzyme in the most sensitive region of its kinetic response to substrate and effector concentrations. This led us to design a multicompound, multisample screening protocol that allows comparison of large numbers of experiments in a single run to minimize systematic sources of error such as changes in enzyme specific activity over time. Ultimately, we decided upon a kinetic screen in which YPK activity was monitored in the presence of compound ± 1 mM FBP using a 96-well plate reader. This screen had the advantage that the activity of each compound was directly assessed and had the added advantage that reaction volumes were 100 µL. The small path length of 100 µL effectively reduced the overall absorbance, which was an advantage since some of the compounds absorb strongly at 340 nm.

Novel Allosteric Effectors of YPK. Approximately one-third of the compounds tested in the initial kinetic screens displayed some kinetic effect under the assay conditions used but were not pursued due to cost and instrumentation constraints. The three compounds studied in detail were chosen on the basis of their particularly strong effect in initial kinetic screens and nonpolar structures (CPDP and HPTP) or its similarity to FBP and known role as an important metabolic intermediate in plants (ribulose-1,5-bisphosphate). This latter compound is the rate-limiting intermediate in the carbon fixation (Calvin) cycle and the substrate for Rubisco (ribulose-1,5-bisphosphate carboxylase).

Ribulose-1,5-bisphosphate (RBP) clearly binds to the same site as FBP, as demonstrated by tryptophan fluorescence binding assays and its dependence on bound divalent cation and substrate for maximum affinity. In the ACD model of RBP, the distance between its phosphates is very near the structurally determined distance between the 1′- and 6′-phosphates of bound FBP, permitting a reasonable and low-energy DOCK solution that places both phosphates in proper binding environments. This result clearly illustrates the rather serendipitous nature of DOCK screens using nonflexible ligand models; relatively small changes in torsion angles along the sugar backbone would have prevented identification of this molecule as an enzyme effector. RBP probably acts as a very weak activator of YPK because of its chemical similarity to FBP. RBP is known to inhibit green algal chloroplast PK (*35*). However, this work was unknown to us at the time RBP was selected in the DOCK screen.

The remaining two compounds described in this paper (CPDP and HPTP) are similar to one another in terms of their chemistry and mechanism of action. First, their DOCKED orientations include contacts to the same general groups in the target allosteric site; second, they are both hydrophobic and have limited solubility in aqueous solution; and third, they display micromolar dissociation constants to YPK and have weak yet measurable activity as allosteric activators. In contrast to the allosteric activator FBP, which achieves its full binding affinity primarily through polar interactions to its terminal phosphate groups, these two compounds appear to bind their receptor site through complementary van der Waals interactions. Whereas RBP

clearly interacts with the FBP site, via polar and electrostatic interactions, the precise location of the CPDP and HPTP binding site or their precise orientation within that site is less well characterized. Since they are acting as weak activators of enzyme activity rather than as inhibitors, it seems likely that we can exclude their direct interaction with the substrate binding site. The fact that CPDP fails to activate the T403E YPK mutant described above implies that this compound does bind to the FBP site.

In contrast, HPTP activates T403E PK. Two interpretations seem equally likely to explain this result: first, the compound may bind to an undetermined site on the enzyme and produce an allosteric effect similar to FBP; or second, HPTP may bind to the FBP site in a manner not precluded by the glutamic acid at position 403. Since the compound is uncharged, electrostatic repulsion terms that contribute to preventing activation by phosphate-containing compounds should not be as strong for HPTP.

In conclusion, structure-based computational methods, using the DOCK suite of programs to screen a large database of small molecular structures, were shown to be a powerful tool in identifying previously unknown or uncharacterized allosteric effectors of a metabolic enzyme. We have shown that it is possible to identify compounds with affinities to the target site that are comparable to those displayed by the natural effector. In addition, while the natural effector and its binding site are significantly polar, it is possible to identify compounds that are uncharged, moderately hydrophobic, and capable of interacting with the binding site. A structural analysis of the enzyme complex with these compounds will be necessary to precisely describe the interactions formed in the allosteric site and their similarity or departure from those modeled in DOCK.

For regulatory sites, the potential kinetic effects of a bound ligand are perhaps more varied than those of a substrate analogue bound to an active site. While the latter type of compounds would generally be expected to act as competitive inhibitors, novel ligands that bind a regulatory site might act either as a mimic or an antagonist of a physiological effector. In addition, the possible effect of such compounds on substrate affinity, on maximal velocity, and on enzyme cooperativity might be separable and distinct. The three compounds described in this paper all seem to act as very weak activators of PK that bind with low to moderate affinity to the FBP site. Such results could be caused by our use of the high-affinity, activated structure of YPK as a target for docking. This could have led us to preferentially select ligands that stabilize the activated enzyme conformation. Because the allosteric site undergoes a disordered to ordered structural transition upon FBP binding, it would be very difficult to test this possibility by screening for ligands specific to the unactivated conformation of the enzyme. A more detailed analysis of this result may require a similar study using a different enzyme with well-ordered structures in the presence and absence of bound effector.

and advice from Dr. Connie Oshiro in the same lab.

REFERENCES

1. Eigenbrodt, E., Reinacher, M., Scheefers-Borchel, U., Scheefers, H., and Friis, R. (1992) Double role for pyruvate kinase type M2 in the expansion of phosphometabolite pools found in tumor cells, *Crit. Rev. Oncog. 3*, 91−115.
2. Mazurek, S., Boschek, C. B., and Eigenbrodt, E. (1997) The role of phosphometabolites in cell proliferation, energy metabolism and tumor therapy, *J. Bioenerg. Biomemb. 29*, 315−330.
3. van Veelen, W. M., and Staal, E. J. (1985) in *Markers of Human Neuroectodermal Tumors* (Staal, E. J., and van Veelen, W. M., Eds.) pp 63−83, CRC Press, Boca Raton, FL.
4. Weernink, A., Rijksen, G., van der Heijden, M. C. M., and Staal, G. E. J. (1990) Phosphorylation of pyruvate kinase type K in human gliomas by a cyclic adenosine 5′-monophosphate-independent protein kinase, *Cancer Res. 50*, 4604−4610.
5. Rijksen, G., van der Heijden, M. C., Oskam, R., and Staal, G. E. J. (1988) Subunit-specific phosphorylation of pyruvate kinase in medullary thyroid carcinomas of the rat, *FEBS Lett. 233*, 69−73.
6. Guminska, M., Ignacak, J., Kedryna, T., and Stachurska, M. B. (1997) Tumor-specific pyruvate kinase isoenzyme M2 involved in biochemical strategy of energy generation in neoplastic cells, *Acta Biochim. Pol. 44*, 711−724.
7. Balinsky, D., Platz, C. E., and Lewis, J. W. (1983) Isozyme patterns of normal, benign, and malignant human breast tissues, *Cancer Res. 43*, 5895−5901.
8. Laughlin, L. T., and Reed, G. H. (1997) The monovalent cation requirement of rabbit muscle pyruvate kinase is eliminated by substitution of lysine for glutamate 117, *Arch. Biochem. Biophys. 348*, 262−267.
9. Early, C. N., and Britt, B. M. (1998) Sequence similarities of glyceraldehyde-3-phosphate dehydrogenases, phosphoglycerate kinases, and pyruvate kinases are species optimal temperature-dependent, *Eur. Biophys. J. 27*, 409−410.
10. Ernest, I., Opperdoes, F. R., and Michels, P. A. (1994) Cloning and sequence analysis of the gene encoding pyruvate kinase in *Trypanoplasma borelli*, *Biochem. Biophys. Res. Commun. 201*, 727−732.
11. Fothergill-Gilmore, L. A., Rigden, D. J., Michels, P. A. M., and Phillips, S. E. V. (2000) Leishmania pyruvate kinase: the crystal structure reveals the structural basis of its unique regulatory properties, *Biochem. Soc. Trans. 28*, 186−190.
12. Mattevi, A., Bolognesi, M., and Valentini, G. (1996) The allosteric regulation of pyruvate kinase, *FEBS Lett. 389*, 15−19.
13. Jurica, M. S., Heath, P. J., Shi, W., Mesecar, A. D., and Stoddard, B. L. (1997) The allosteric regulation of pyruvate kinase by fructose-1,6-bis-phosphate, *Nat. Struct. Biol 6,* 195−210.
14. Johannes, K.-J., and Hess, B. (1973) Allosteric kinetics of pyruvate kinase of *Saccharomyces carlsbergensis*, *J. Mol. Biol. 76*, 181−205.
15. Ikeda, Y., and Noguchi, T. (1998) Allosteric Regulation Of Pyruvate Kinase M-2 Isozyme Involves a Cysteine Residue In the Intersubunit Contact, *J. Biol. Chem. 273*, 12227−12233.
16. Noguchi, T., Inoue, H., and Tanaka, T. (1986) The M1 and M2-type isozymes of rat pyruvate kinase are produced from the same gene by alternative RNA splicing, *J. Biol. Chem. 261*, 13807−13812.
17. Allen, S. C., and Muirhead, H. (1996) Refined three-dimensional structure of cat-muscle (M1) pyruvate kinase at a resolution of 2.6 Å, *Acta Crystallogr. D52*, 499−504.
18. Muirhead, H., Clayden, D. A., Barford, D., Lorimer, C. G., Fothergill-Gilmore, L. A., Schiltz, E., and Schmitt, W. (1986) The structure of cat muscle pyruvate kinase, *EMBO J. 5*, 475−481.
19. Stuart, D. I., Levine, M., Muirhead, H., and Stammers, D. K. (1979) Crystal structure of cat pyruvate kinase at a resolution of 2.6 Å, *J. Mol. Biol. 134*, 109−142.
20. Larsen, T. M., Laughlin, T., Holden, H. M., Raymont, I., and Reed, G. H. (1994) Structure of rabbit muscle pyruvate kinase complexed with Mn^{2+}, K^+, and pyruvate, *Biochemistry 33*, 6301−6309.
21. Mattevi, A., Valentini, G., Rizzi, M., Speranza, M. L., Bolognesi, M., and Coda, A. (1995) Crystal structure of *Escherichia coli* pyruvate kinase type I: molecular basis of the allosteric transition, *Structure 3*, 729−741.
22. Mesecar, A. D., and Nowak, T. (1997) Metal-ion-mediated allosteric triggering of yeast pyruvate kinase. 1. A multidimensional thermodynamic linked-function analysis, *Biochemistry 36*, 6803−6813.
23. Mesecar, A. D., and Nowak, T. (1997) Metal-ion-mediated allosteric triggering of yeast pyruvate kinase. 2. A multidimensional thermodynamic linked-function analysis, *Biochemistry 36*, 6803−6813.
24. Shoichet, B. K., and Kuntz, I. D. (1993) Matching chemistry and shape in molecular docking. *Protein Eng. 6*, 723−732.
25. Shoichet, B. K., Stroud, R. M., Santi, D. V., Kuntz, I. D., and Perry, K. M. (1993) Structure-based discovery of inhibitors of thymidylate synthase, *Science 259*, 3493−3497.
26. Meng, E. C., Shoichet, B. K., and Kuntz, I. D. (1992) Automated docking with grid-based energy evaluation, *J. Comput. Chem. 13*, 505−524.
27. Kuntz, I. D., Meng, E. C., and Shoichet, B. K. (1994) Structure-based molecular design, *Acc. Chem. Res. 27*, 117−123.
28. Ferrin, T. E., Huang, C. C., Jarvis, L. E., and Langridge, R. (1988) The MIDAS display system, *J. Mol. Graphics 6*, 13−27.
29. *QUANTA molecular modeling program* (1996) Molecular Simulations, Inc., San Diego CA.
30. *Available Chemicals Directory* (1997), MDL Inc., San Leandro CA.
31. Fishbein, R., Benkovic, P. A., and Benkovic, S. J. (1975) The anomeric specificity of yeast pyruvate kinase toward the activation by D-fructose-1,6-bisphosphate. *Biochemistry 14*, 4060−4063.
32. Pierce, J., Serianni, A. S., and Barker, R. (1985) Anomerization of furanose sugars and sugar phosphates. *J. Am. Chem. Soc. 107*, 2448−2456.
33. Wurster, B., and Hess, B. (1976) Tautomeric and anomeric specificity of allosteric activation of yeast pyruvate kinase by D-frucose-1,6-bisphosphate and its relevance in D-glucose catabolism. *FEBS Lett. 63*, 17−21.